EPR Line Shifts and Line Shape Changes Due to Spin Exchange of Nitroxide Free Radicals in Liquids

Barney L. Bales* and Miroslav Peric

Department of Physics and Astronomy and The Center for Cancer and Developmental Biology, California State University at Northridge, Northridge, California 91330

Received: March 19, 1997; In Final Form: July 22, 1997[⊗]

An expression for the EPR line shape of a nitroxide free radical undergoing spin exchange in the slow exchange limit is derived and tested experimentally and against a rigorous theory. The line shape is the sum of the absorption and dispersion of Lorentzian lines, in which the dispersion component is of opposite signs for the outer lines and zero for the inner. The relative amplitude of the absorption and the dispersion is shown to be a linear function of the spin exchange frequency. Nonlinear least-squares fitting of the spectra allows the separation of the absorption and dispersion components determining their relative amplitudes to high precision yielding values of the spin exchange frequency that are of precision comparable to those derived from the more traditional line broadening. This new way to measure spin exchange frequencies is attractive because there are no complications from dipolar interactions and no measurements at low concentrations are required. The resonance fields of the absorption component of the outer lines shift toward the center of the spectrum as the square of the spin exchange frequency and the observed positions of the lines shift even further due to the absorption−dispersion overlap. The observed shift is also a quadratic function of the spin exchange frequency and involves the unbroadened line width. Both shifts may be used to measure the spin exchange frequency; however, only the observed shift yields values that are of precision comparable with broadening and dispersion-amplitude techniques. The predictions of the theory are tested experimentally using peroxylamine disulfonate in 50 mM K_2CO_3 at 67 °C. At this elevated temperature, the concentration of the radical decreases at a convenient rate making it possible to study a wide concentration range without disturbing the sample. The line broadening was linear with the concentration with a coefficient of correlation $r = 0.99996$. The spin exchange frequency derived from the amplitude of the dispersion component was within less than 1% of that derived from line broadening and of comparable precision. Spin exchange frequencies derived from the shift of the lines were of lower precision yielding values of the spin exchange frequency about 2% lower than those found from line broadening.

Introduction

It has been 37 years since Daniel Kivelson first published[1] a theory to describe spin exchange between free radicals in liquids. During these 37 years, much theoretical[2−9] and experimental[3,7,10−19] work has been devoted to the EPR spectral changes induced by spin exchange between radicals in liquids. A monograph[4] published in English in 1980 gathered a wealth of theoretical and experimental data and described the use of the spin exchange technique to study problems in chemistry and biology.

The present work is restricted to the case of spin exchange between identical ^{14}N nitroxide free radicals undergoing rapid translational and rotational motion. At negligible spin exchange frequencies, the EPR spectrum is composed of three well-separated narrow hyperfine lines. The well-known qualitative features of the effect of spin exchange which are illustrated in the textbooks (for example, in Figure 9-4, p 202, of ref 20) are as follows: as the spin exchange frequency increases, the three lines broaden and move toward the center at spin exchange frequencies small compared with the line separation, the so-called slow exchange limit. At higher spin exchange frequencies, the lines broaden further and coalesce into one broad line; and finally at still higher frequencies, the broad line narrows. All of these effects are predicted by various theories,[2−9] and all of them have been observed experimentally.[3,7,10−19] The original theory due to Kivelson[1] was based upon the general theory of motional narrowing due to Kubo and Tomita[21] and was able to predict the effects of spin exchange in the two limits of slow exchange and narrowing but could not describe the entire range. A rigorous theory covering the entire range was given by Currin[6] in 1962, and the modified Bloch equations were employed by Jones[3] the following year. Another rigorous theory, clarifying the physical significance of some of the assumptions of Currin and eliminating the need for others was given by Freed[2] in 1966, and a similar treatment was given the following year by Johnson.[8]

It is known that, in principle, the spin exchange frequency may be deduced by studying line narrowing, line shifts, or line broadening.

For nitroxides, extreme line narrowing has been studied in liquids only once,[17] yielding spin exchange frequencies in agreement with those derived from line broadening. As a practical matter, observation of spin exchange narrowing in liquids requires concentrations far too high to make it useful as a tool to study most interesting systems. There are other problems as well as is discussed on pp 117−119 of ref 4. Thus, even though the study of line narrowing was important in order to confirm that aspect of the theory, it is not a promising technique especially in biology.

Line shifts in nitroxides have been carefully studied only once, by Jones,[3] using a modified Bloch equation formulation to analyze the data. Excellent agreement between spin exchange frequencies derived from line broadening and line shifts was

* Electronic mail: barney.bales@csun.edu. FAX 818 677 3234.

[⊗] Abstract published in *Advance ACS Abstracts,* October 1, 1997.

S1089-5647(97)00995-4 CCC: $14.00

obtained. Line shifts in the spectra due to aqueous solutions of $VOSO_4$ have been analyzed using the theory of Molin et al. (see p 116 of ref 4) again confirming the theory, unfortunately with an uncertainty that was 50% of the result. Thus, even though the studies of line shifts were important in order to confirm that aspect of the theory, they have not been used as routine techniques.

Almost all of the experimental determinations of the spin exchange frequency to date have been based upon line broadening rather than line shifts because the former could be determined with higher precision than the latter. Three recent developments have changed the situation. First, magnetic field sweep units exhibiting extraordinary linearity and short-term reproducibility have become available. Second, detailed understanding of the effect of inhomogeneous broadening on the nitroxide EPR line shapes has been achieved leading to accurate representations of the EPR line shape.[22] This allows nonlinear least-squares fitting techniques[23,24] to be used which in turn permits the location and intrinsic line width of a resonance line to be determined with high precision even with rather noisy spectra. Third, it has been learned that modulation broadening contributes only to the Gaussian component of the resonance lines[25] which means that improved signal-to-noise ratios may be obtained by modulation broadening the lines while maintaining high precision in determining intrinsic line widths and positions.

The general theories are essentially equivalent when applied to nitroxide free radicals that show no inhomogeneous broadening. Some of these theories predict complex eigenvalues, which implies a mixture of absorptive and dispersive components that distorts the line shape from Lorentzian. This aspect of spin exchange has not been studied experimentally yet. Molin et al.[4] applied a second-order perturbation analysis to their theory in the slow exchange limit to produce more accurate analytical expressions. Following their development, we show that the distortion is due to the introduction of what we have called spin exchange induced dispersion into the outer lines of the spectrum from which yet another, independent measure of the spin exchange frequency may be obtained in principle.

The purpose of the present work is as follows: (1) to critically test the predictions of the theory of Molin et al.[4] and define the limits of its applicability, (2) to test the theoretical prediction of a spin exchange induced dispersion and to learn if it is practical to measure the spin exchange frequency from this effect, and (3) to critically assess the precision with which line shifts may be used to derive spin exchange frequencies.

In addition to the interest inherent to the stated purposes, there are practical motivations to the work. First, dipolar interactions, important in experiments at small T/η, where T is the absolute temperature and η is the viscosity, also broaden the lines in proportion to the concentration.[4,10,15,16,18] In those experiments, the broadening due to dipolar and spin exchange interactions must be separated before conclusions may be drawn. This separation is not straightforward at constant temperature. Second, there are experimental situations in which line broadening is not straightforward to analyze. These points are discussed below.

Peroxylamine disulfonate (PADS) in 50 mM K_2CO_3 studied at 67 °C was chosen for this first study because complications due to inhomogeneous broadening are absent rendering lines that are very nearly Lorentzian in the absence of spin exchange. The dianion radical of PADS is unstable, and we exploit this fact to vary the radical concentration by carrying out the experiment at an elevated temperature. This has three advantages: first, the sample is undisturbed during the experiment

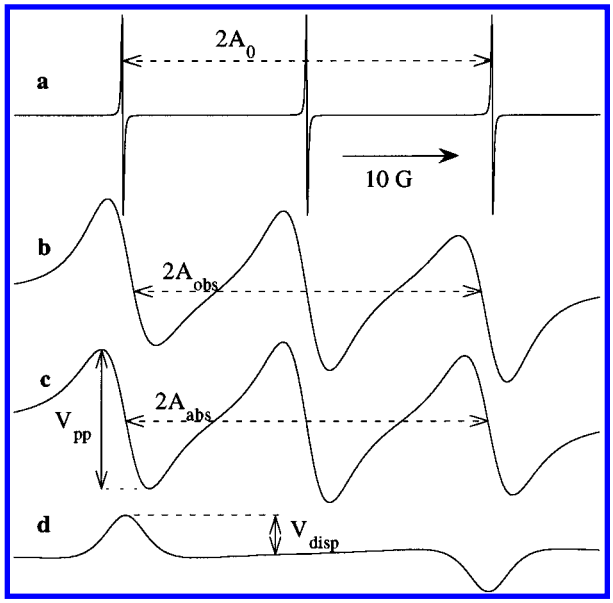

Figure 1. Simulated EPR spectra of a nitroxide radical with $A_0 = 15.8285$ G and $\Delta H^{L}_{pp}(0)_{M_I} = 0.123$ G undergoing spin exchange at frequency (a) $\omega_{ex}/\gamma = 0$ and (b) $\omega_{ex}/\gamma = 5.19615$ G ($\omega_{ex}/\gamma A_0 = 0.3283$). The best fit of eq 11 to the spectrum in (b) is essentially perfect if the intensity, I_{M_I}, is allowed to vary and the two terms in eq 11 are displayed in (c) the absorption and (d) the spin exchange induced dispersion. A_{obs} is one-half the distance between the outer lines. A_{abs} is the distance between the resonance fields of the outer lines of the absorption component. $A_{obs} < A_{abs}$ because the overlap of the dispersion lines shift the observed lines further than the shift of the resonance fields. The pertinent amplitudes V_{pp} and V_{disp} are defined.

permitting precise relative measurements of the signal intensity; second, the concentration of dissolved salts is constant; and third, the value of $T/\eta = 8 \times 10^4$ K/P is well above the values of $T/\eta = 5 \times 10^3$ K/P, below which dipolar interactions affect the spectra.[10] In this experiment, the precise absolute radical concentration is not of interest, only the relative concentrations that are accurately deduced from fitting the observed spectra to an appropriate line shape.

Theory

We restrict the discussion to cases in which nitroxide free radical tumbles rapidly producing motionally narrowed EPR spectra. Figure 1a shows such a three-line spectrum in the absence of spin exchange, defining the ^{14}N hyperfine coupling constant, A_0. Figure 1b shows the effect of spin exchange such that $\omega_{ex} = 0.3283\ \gamma A_0$ which crowds the upper limit of the so-called slow exchange case defined by $\omega_{ex} \ll \gamma A_0$. Here, ω_{ex} is the spin exchange frequency and γ the gyromagnetic ratio of the electron. The three lines are denoted by their values of the ^{14}N spin quantum number, $M_I = +1$, 0, and -1 corresponding respectively to the low-, middle-, and high-field lines.

In the absence of unresolved hyperfine structure, the resonance lines have the Lorentzian shape, and for the slow exchange limit, all of the theories[2−4,8,10,19] predict that spin exchange broadens the lines as follows:

$$B_{M_I} = 4\omega_{ex}/3\sqrt{3}\gamma \qquad (1)$$

where the broadening, B_{MI} , is defined to be

$$B_{M_I} = \Delta H^{L}_{pp}(\omega_{ex})_{M_I} - \Delta H^{L}_{pp}(0)_{M_I} \qquad (2)$$

The broadening is predicted to be independent of M_I; however, we retain the dependence on M_I for reasons discussed

below. In eq 2, $\Delta H^{L}_{pp}(\omega_{ex})_{M_I}$ is the Lorentzian peak-to-peak line width of the M_I line at spin exchange frequency ω_{ex}, and the zero indicates this line width in the limit of zero spin exchange (zero concentration). According to eq 1, the broadening of the lines in Figure 1b is expected to be 4.00 G. Direct measurement of the widths of the three lines yields $B_{+1} = B_{-1} = 4.59$ G and $B_0 = 3.88$ G, yielding an average broadening of 4.35 G, about 8.8% higher than the prediction of eq 1.

Most nitroxide spectra are accurately described by the Voigt shape, which is a Lorentzian−Gaussian convolution; however, we consider only Lorentzian lines in this paper for several reasons. First, the experimental measurements are made using a radical that very nearly yields a Lorentzian line shape at low spin exchange frequencies. Second, the new interesting results appear at spin exchange frequencies large enough that inhomogeneous broadening has only a minor effect. Finally, methods[22,26−28] are available to separate the Gaussian and Lorentzian components if need be.

Experimentally, ω_{ex} may be controlled by exploiting the fact that ω_{ex} is proportional to the concentration,[2−4,8,10,19] thus

$$\omega_{ex} = K[\text{PADS}] \tag{3}$$

where [PADS] is the molar concentration of PADS and the factor K depends on the temperature, viscosity, charge of the nitroxide, ionic strength,[13] and perhaps steric factors.[4] To the extent that PADS influences the viscosity and the ionic strength, K could show some dependence upon [PADS]; in fact, Eastman et al.[13] found that K varied as $[\text{PADS}]^{m'}$ with $m' = 0.17 \pm 0.03$ using concentrations up to [PADS] = 57 mM, while Jones[3] reported $m' = 0.07 \pm 0.02$ using concentrations up to [PADS] = 80 mM. Later, Eastman[29] reported data up to [PADS] = 56 mM which were fit to $m = 0$. The behavior of K with temperature, viscosity, and ionic strength, studied by Eastman et al.,[13] is not of concern in this work. Our concern was to minimize the dependence of K on [PADS] by holding these three variables constant; i.e., to ensure that $m' \approx 0$. The temperature is held constant, and the viscosity and ionic strength are not expected to vary significantly since the concentration of PADS plus products is constant. Often, the Stokes−Einstein relation holds:

$$K = \text{constant}\cdot T/\eta \tag{4}$$

where T is the absolute temperature and η the shear viscosity; however, this is not necessary to reach the conclusions of this work.

The EPR line shape of a radical undergoing slow exchange; i.e., $\omega_{ex} \ll \gamma A_0$ is given by eq 2.81 of Molin et al.,[4] which may be rewritten as a function of the magnetic field, H, as follows:

$$Y_{M_I}(H,\omega_{ex}) = \frac{2I_{M_I}}{\pi\Delta H^{L}_{1/2}(\omega_{ex})_{M_I}} \frac{(1 + b_{M_I}\xi_{M_I})}{[1 + \xi_{M_I}{}^2]} \tag{5}$$

where I_{M_I} is the integrated intensity, $\Delta H^{L}_{1/2}(\omega_{ex})_{M_I}$ is the line width at half-height (the superscript denotes Lorentzian), and

$$\xi_{M_I} = 2\frac{H - H(\omega_{ex})_{M_I}}{\Delta H^{L}_{1/2}(\omega_{ex})_{M_I}} \tag{6}$$

The subscript M_I labels the ^{14}N hyperfine line which appears at resonance field $H(\omega_{ex})_{M_I}$. The coefficients b_{M_I} are computed by Molin et al.[4] (p 47 above eq 2.86) as follows:

$$b_{M_I} = -2(\omega_{ex}/\gamma) \sum_{M_I' \neq M_I} \frac{\phi_{M_I'}}{H(0)_{M_I} - H(0)_{M_I'}} \tag{7}$$

where the sum is over the two nuclear quantum numbers other than M_I and $\phi_{M_I'}$ is the statistical weight of the spins in this configuration; $\phi_{M_I'} = {}^1/_3$ for ^{14}N nitroxides. [In the orginal notation, $b_{M_I} = v_k/u_k$, where the subscript k labels the line. This ratio v_k/u_k is found from the equations immediately preceding eq 2.86.] The zero indicates the resonance fields in the limit of zero spin exchange (zero concentration). The three lines comprising the spectrum are equally separated by the nitrogen hyperfine coupling constant, A_0, if we neglect the small second-order shift,[30] $A_0{}^2/2H(0)_0$. Neglecting this quantity, eq 7 yields $\omega_{ex}/\gamma A_0$ for $M_I = 1$, $-\omega_{ex}/\gamma A_0$ for $M_I = -1$, and zero for $M_I = 0$. These results may be summarized for any of the three lines by

$$b_{M_I} = M_I\omega_{ex}/\gamma A_0 \tag{8}$$

The first derivative of eq 5 with respect to H is given by

$$Y'_{M_I}(H,\omega_{ex}) = \frac{-8\sqrt{3}I_{M_I}}{\pi[\Delta H^{L}_{pp}(\omega_{ex})_{M_I}]^2} \frac{\left\{\xi'_{\mathbf{M}_I} - \frac{\sqrt{3}b_{M_I}}{6}[3 - \xi'_{M_I}{}^2]\right\}}{[3 + \xi'_{M_I}{}^2]^2} \tag{9}$$

where

$$\xi'_{M_I} = 2\frac{H - H(\omega_{ex})_{M_I}}{\Delta H^{L}_{pp}(\omega_{ex})_{M_I}} \tag{10}$$

and $\Delta H^{L}_{pp}(\omega_{ex})_{M_I} = \Delta H^{L}_{1/2}(\omega_{ex})_{M_I}/\sqrt{3}$ is the peak-to-peak line width in the first derivative spectrum.

The spectrum described by eq 9 is composed of the familiar Lorentzian absorption plus a term that has the mathematical form of the dispersion of a Lorentzian whose intensity varies with ω_{ex} and sign varies with M_I. The second integral of eq 9 with respect to H is the signal intensity, I_{M_I}, which is expected to be independent of M_I for any practical temperature; i.e., the three lines are equally intense. Nevertheless, we retain the dependence of I_{M_I} on M_I for reasons discussed below. The dispersion term does not contribute to I_{M_I} and does not represent an absorption of energy. The sum of eq 9 over the three values of M_I yields the predicted spectrum:

$$Y'(H,\omega_{ex}) = \sum_{M_I} I_{M_I}[L^{A}_{M_I}I(H) + D^{A}_{M_I}(H)] \tag{11}$$

with the Lorentzian absorption $L^{A}_{M_I}$ of unit doubly integrated intensity given by

$$L^{A}_{M_I}(H) = \frac{-8\sqrt{3}}{\pi[\Delta H^{L}_{pp}(\omega_{ex})_{M_I}]^2} \frac{\xi'_{M_I}}{[3 + \xi'_{M_I}{}^2]^2} \tag{12}$$

and the spin exchange induced dispersion given by

$$D^{A}_{M_I}(H) = \frac{4b_{M_I}[3 - \xi'_{M_I}{}^2]}{\pi[\Delta H^{L}_{pp}(\omega_{ex})_{M_I}]^2[3 + \xi'_{M_I}{}^2]^2} \tag{13}$$

The superscript A refers to the fact that the absorption term is normalized to unit intensity (area).

Amplitude of the Spin Exchange Dispersion

It is convenient to rewrite eq 9 in terms of the peak-to-peak height of the absorption component, V_{pp}, and the maximum amplitude of the spin exchange dispersion component, V_{disp}, as follows:

$$Y'_{M_I}(H,\omega_{ex}) = \frac{\{-8V_{pp}(M_I)\xi'_{M_I} + 3V_{disp}(M_I)[3 - \xi'^{2}_{M_I}]\}}{[3 + \xi'^{2}_{M_I}]^2} \tag{14}$$

where

$$V_{pp}(M_I) = \sqrt{3}I_{M_I}/\pi[\Delta H^{L}_{pp}(\omega_{ex})_{M_I}]^2 \tag{15}$$

$$V_{disp}(M_I) = 4V_{pp}(M_I)\frac{\sqrt{3}b_{M_I}}{9} \tag{16}$$

Therefore, the spectrum may be written

$$Y'(H,\omega_{ex}) = \sum_{M_I}[V_{pp}(M_I)L'_{M_I}(H) + V_{disp}(M_I)D'_{M_I}(H)] \tag{17}$$

with the Lorentzian absorption of unit peak-to-peak height given by

$$L'_{M_I}(H) = \frac{-8\xi'_{M_I}}{[3 + \xi'^{2}_{M_I}]^2} \tag{18}$$

and the spin exchange induced dispersion of unit maximum amplitude given by

$$D'_{M_I}(H) = \frac{3[3 - \xi'^{2}_{M_I}]}{[3 + \xi'^{2}_{M_I}]^2} \tag{19}$$

Combining eqs 8 and 16, we find

$$V_{disp}(M_I)/V_{pp}(M_I) = M_I\frac{4\omega_{ex}}{3\sqrt{3}\gamma A_0} \tag{20}$$

Utilizing eq 1, eq 20 may be written

$$V_{disp}(M_I)/V_{pp}(M_I) = M_I B(M_I)/A_0 \tag{21}$$

Note that eq 21 supposes that the broadening $B(M_I)$ is due to spin exchange and not some other concentration-dependent broadening such as dipolar and might provide a test of this supposition in situations in which dipolar broadening is suspected. [The assumption that dipolar interactions do not modify the line shape is based upon simple motional narrowing theory[10,18] ignoring dynamic frequency shifts. In viscous liquids, there may be complications in the role of dipolar interactions.]

Therefore, the magnitude of the relative amplitudes of the Lorentzian absorption and the spin exchange-induced dispersion yields the spin exchange frequency, (eq 20). Note that according to eq 21, the relative amplitudes of the absorption and dispersion terms in eq 17 is the broadening divided by the hyperfine coupling constant with a positive sign for the low-field line and a negative sign for the high-field line. The center line shows no spin exchange dispersion. This latter fact is convenient experimentally because it provides a means to correct for the "normal" dispersion; i.e., the detected magnetization that varies in phase with the microwave field. Normal dispersion is often encountered experimentally, especially with aqueous samples.[31]

Shift of Hyperfine Lines

It is well-known that exchange between sites of different resonance frequency shifts those resonance frequencies toward one another. An interesting perspective is provided by Slichter[32] (p 593). Many authors, using many different theoretical techniques, have addressed the problem; however, other than Molin et al.,[4] it does not seem to be widely appreciated that the observed shift is the sum of two contributions. First, the resonance field $H(0)_{M_I}$ shifts to $H(\omega_{ex})_{M_I}$ upon onset of spin exchange. Second, the overlap of the dispersion component shifts the position of the observed line further. Compare Figures 1b and 1c.

The shift of $H(0)_{M_I}$ is given by eq 2.83 of Molin et al.[4] as

$$H(\omega_{ex})_{M_I} - H(0)_{M_I} = \phi_{M_I}(\omega_{ex}/\gamma)^2 \sum_{M'_I \neq M_I} \frac{\phi_{M'_I}}{H(0)_{M'_I} - H(0)_{M_I}} \tag{22}$$

The sum is evaluated as in eq 7 yielding

$$H(\omega_{ex})_{M_I} - H(0)_{M_I} = M_I\frac{1}{6A_0}(\omega_{ex}/\gamma)^2 \tag{23}$$

Therefore, the low-field absorption component ($M_I = +1$) is shifted upfield, the high-field line downfield, while the center line is unaffected. The shift expressed by eq 23 is illustrated in Figure 1 as the shift of the absorption component, Figure 1c from the original line positions, Figure 1a, but is not the measured shift. This is because, as pointed out by Molin et al.,[4] the superposition of the spin exchange dispersion components shifts the lines further to positions $H(\omega_{ex})^{obs}_{M_I}$, which are defined as the positions that the observed resonances are at their maxima or where the first derivatives cross the baseline. The second shift, which is given by eq 2.86 in Molin et al.,[4] involves $\Delta H^{L}_{pp}(0)_{M_I}$ and the sum that appears in eq 22. Writing their expression in terms of a first derivative, field-swept presentation and adding to eq 23 yields

$$H(\omega_{ex})^{obs}_{M_I} - H(0)_{M_I} = \frac{M_I}{2}\left[\frac{\sqrt{3}}{2}\Delta H^{L}_{pp}(0)_{M_I} + \frac{\omega_{ex}}{\gamma}\right]\frac{\omega_{ex}}{\gamma A_0} \tag{24}$$

[Equation 24 is equivalent to eq 3.24 in Molin's book.] It is convenient to measure the distance between the $M_I = +1$ and -1 lines in the spectrum. If we define $2A_{abs} = [H(\omega_{ex})_{-1} - H(\omega_{ex})_{+1}]$ and $2A_{obs} = [H(\omega_{ex})^{obs}_{-1} - H(\omega_{ex})^{obs}_{+1}]$ from eqs 23 and 24, we find

$$A_{abs} = A_0 - \frac{1}{6A_0}(\omega_{ex}/\gamma)^2 \tag{25}$$

$$A_{obs} = A_0 - \frac{1}{2}\left[\frac{\sqrt{3}}{2}\Delta H^{L}_{pp}(0)_{\pm 1} + \frac{\omega_{ex}}{\gamma}\right]\frac{\omega_{ex}}{\gamma A_0} \tag{26}$$

where $\Delta H^{L}_{pp}(0)_{\pm 1}$ denotes the average Lorentzian line width of the $M_I = +1$ and -1 lines in the absence of spin exchange. Equation 26 is one-half the distance between the low- and high-field lines, directly measurable from the EPR spectrum; eq 25 is one-half the distance between the resonance fields of the absorption components of the low- and high-field lines which must be found by fitting of eqs 11 or 17 to the experimental

TABLE 1: Accuracy of Eqs 1, 20, 25, and 26 at a High Exchange Frequency, $\omega_{ex}/\gamma A_0 = 0.3283$[a]

method used to measure parameter	parameter[b]	value	eq	% error in ω_{ex}[c]
direct measurement from the spectrum	A_{obs}/A_0	0.939 07	26	5.0
	$B_{\pm1}$	4.59 G	1	14.8
	B_0	3.88 G	1	−3.0
	$\langle B_{M_I}\rangle$	4.35 G	1	8.8
least-squares fit to Lorentzian; intensities of the three lines constrained to be the same	A_{obs}/A_0	0.942 98	26	1.5
	$B_{\pm1}$	4.17 G	1	4.3
	B_0	3.95 G	1	−1.3
	$\langle B_{M_I}\rangle$	4.10 G	1	2.5
least-squares fit to eq 11 or 17; intensities of the three lines constrained to be the same	$\lvert V_{disp}(\pm1)/V_{pp}(\pm1)\rvert$	0.262	20	3.5
	A_{abs}/A_0	0.981 27	25	2.1
	$B_{\pm1}$	4.10 G	1	2.5
	B_0	3.77 G	1	−5.7
	$\langle B_{M_I}\rangle$	3.99 G	1	−0.3
least-squares fit to eq 11 or 17; intensities of the three lines allowed to vary; $I(\pm1) = 0.893I(0)$	$\lvert V_{disp}(\pm1)/V_{pp}(\pm1)\rvert$	0.267	20	5.7
	A_{abs}/A_0	0.981 90	25	0.4
	$B_{\pm1}$	4.03 G	1	0.6
	B_0	3.95 G	1	−1.2
	$\langle B_{M_I}\rangle$	4.00 G	1	0.0

[a] Input parameters: $A_0 = 15.8285$ G, $\omega_{ex}/\gamma = 5.196$ G, and $\Delta H^0_{pp}(M_I) = 0.123$ G. The broadening predicted by eq 1 (all theories) is $B(M_I) = 4.000$ G independent of M_I. [b] B_{M_I} were computed from eq 2 using the input value of $\Delta H^0_{pp}(M_I)$; $\langle B_{M_I}\rangle$ is the average value of B_{M_I}. [c] $100(\omega_{ex}/\gamma - 5.196\text{ G})/5.196$ G, where ω_{ex} is computed from the observed parameter using the equation indicated in the penultimate column.

spectrum. As a practical matter, eq 26 would be used in a routine experiment. Equation 25 is of interest in order to test the theory in detail. It is important to note that the shift often quoted in the textbooks is equivalent to eq 25. It is interesting to note that for small $\Delta H^L_{pp}(0)_{\pm1}$, two-thirds of the observed shift is due to the absorption-dispersion overlap.

Materials and Methods

Fremy's salt (Sigma) and K_2CO_3 (Mallinckrodt) were used as received. Deionized water was distilled twice. The purity of the Fremy's salt was estimated to be 78 ± 4% by comparing spectra from freshly prepared solutions of Fremy's salt and 4-oxo-2,2,6,6-tetramethylpiperidine-d_{17} (perdeuterated Tempone, CDN Isotopes, as received). A sample of PADS in 50 mM K_2CO_3 was prepared at a nominal concentration of 33.5 ± 1.7 mM. The sample was degassed by bubbling a stream of N_2 gas through the sample for 10 min. A sample was sealed into a 50-μL disposable pipet and placed into a quartz tube which was then placed into a Bruker temperature control unit previously stabilized at a set point of 70 °C. This temperature was selected because it produced a decay of the spectrum which was fast enough to carry out the entire experiment in about 1.6 h and was slow enough so that the decay of the spectrum was not significant during one scan.

A thermocouple was placed above the sample in configuration C of Figure 1 of ref 33. After correction for the temperature gradient, the sample temperature was 67 ± 1 °C, stable to within 0.2 °C over the 97 min of the experiment. The temperature uncertainty was dominated by the correction for the gradient; however, since the temperature is irrelevant to the conclusions of this paper, no effort was made to improve the accuracy.

EPR spectra were measured with a Bruker 300 ESP X-band spectrometer interfaced with Bruker's computer. Spectra were acquired every 5 min using a sweep time of 21 s; microwave power, 5 mW; time constant, 5 ms; sweep width, 50 G; modulation amplitude 0.1 G. This modulation amplitude broadened the Gaussian component as expected[25] by $\Delta H^G_{pp} = 0.051 \pm 0.004$ G. The overall Gaussian line width of 0.078 ± 0.008 G was corrected using the methods of ref 22; however, the corrections turned out to be negligible except at low concentrations. The spectra were acquired automatically, retuning automatically before each sweep, and stored on the hard disk using a simple macro within the 300 ESP software supplied by Bruker. Afterward, the spectra were transferred by ethernet to a personal computer for analysis.

Spectra at low concentrations, where spin exchange is minimal, were analyzed by the program Lowfit, which searches for the minimum least-squares difference in the spectrum and a theoretical model of a Gaussian−Lorentzian sum function taking advantage of the fact that such a sum function is an excellent approximation to the Voigt shape.[22,24] Theoretical spectra were simulated from equations given in the Appendix derived from the theory of Currin.[6]

Results

We first compare the results of perturbation theory due to Molin et al.,[4] as applied to nitroxide radicals in eqs 1, 20, 25, and 26, with Currin's[6] theory. Spectra were generated from the equations in the Appendix using input values of ω_{ex}, A_0, and $\Delta H^L_{pp}(0)_{M_I}$. These input values were taken to be the true values, and the predictions of eqs 1, 20, 25, and 26 were tested by treating the theoretical spectra as if they were experimental spectra. The broadening (eq 1) and the observed spacing between the $M_I = -1$ and $+1$ lines, A_{obs} (eq 26) are directly measurable from the spectra. The dispersion−absorption amplitude ratio (eq 20) and the spacing between the $M_I = -1$ and $+1$ absorption components were measured using nonlinear least-squares fitting techniques that have become available[23,24] in recent years. Thus, we found the best fit of eq 11, or equivalently, eq 17 to the theoretical spectra and compared the best fit parameters of those equations to the true values. An example of such a simulation is given in Figure 1b in which $A_0 = 15.8285$ G, $\omega_{ex}/\gamma = 5.19615$ G, and $\Delta H^L_{pp}(0)_{M_I} = 0.123$ G; i.e., $\omega_{ex}/\gamma A_0 = 0.3283$. The example in Figure 1 is an extreme case, with a value of $\omega_{ex}/\gamma A_0$ well above the largest value of $\omega_{ex}/\gamma A_0 \approx 0.11$ encountered in this study. Figures 1c and 1d are plots of the least-squares fit of the two terms comprising eq 11 in which the values of doubly integrated intensities, I_{M_I}, were allowed to vary independently as fit parameters. The fit is essentially perfect; i.e., Figure 1b is indistinguishable from the sum of spectra in Figures 1c and 1d. A fit constraining the values of I_{M_I} to be equal to one another, yields a curve barely distinguishable from Figure 1b (not shown). A fit using only a Lorentzian absorption (not shown) is poor; nevertheless, the results of such a fit are interesting as is discussed below. Table 1 shows the comparison between the true values of ω_{ex} and

TABLE 2: Limit Value of $\omega_{ex}/\gamma A_0$ Yielding <2% Error in ω_{ex}[a]

		fit eq 11		
parameter	direct measurement	$I(M_I)$ constant	$I(M_I)$ varied	fit Lorentzian absorption
$\lvert V_{disp}/V_{pp}\rvert$		0.29	0.21	
A_{abs}/A_0		0.21	>0.41	
A_{obs}/A_0	0.21			0.37[b]
$\langle B_{M_I}\rangle$	0.17	>0.41	>0.41	0.31

[a] Same input values as Table 1. [b] For $\Delta H^0_{pp}(M_I) = 1.0$ G, limit value of $\omega_{ex}/\gamma A_0 = 0.30$ G.

those deduced by various fitting models and by direct measurement. The parameter from which ω_{ex} is derived is indicated in Table 1. Even at a rather large value of $\omega_{ex}/\gamma A_0 = 0.3283$, straightforward measurements of A_{obs} and $B(M_I)$ from the spectrum yield reasonable results: ω_{ex} is in error by only 5% when deduced from A_{obs} and is in error by 8.8% when deduced from the average broadening. Likewise, fitting with a Lorentzian absorption only yields surprisingly good results considering that the fit itself is poor: ω_{ex} is determined to within 1.5% from A_{obs} and to within 2.5% from the average broadening, $\langle B_{M_I}\rangle$. These facts are of practical importance because fitting yields better values of A_{obs} and $B(M_I)$ than direct measurement by an order of magnitude or more depending upon the signal-to-noise.

These results show that the expression for line shifts due to Molin et al.,[4] involving as they do both shifts due to spin exchange directly and shifts due to line-shape distortions indirectly, are in agreement with theory. Jones' treatment is also in agreement with eq 26 in the limit of $\Delta H^L_{pp}(0)_{M_I} = 0$. Turning to the predictions of eqs 20 and 25, Table 1 shows that values of ω_{ex} deduced from $V_{disp}(M_I)/V_{pp}(M_I)$ are within 3.5% and from A_{abs}/A_0 are within 2.1% of the true values when I_{M_I} are constrained to be the same. When deduced from the average broadening, ω_{ex} is in error by an insignificant -0.3% employing the same constraint.

Finally, Table 1 shows that allowing I_{M_I} to vary in the fit of eq 11 or 17 to the theoretical spectrum yields some potentially interesting results at higher spin exchange frequencies. The value of ω_{ex} deduced from A_{abs}/A_0 is within 0.4% of its true value and the average broadening reproduces ω_{ex} exactly. The best-fit intensities of the outer lines are about 11% smaller than the central line leading to values of $V_{disp}(M_I)/V_{pp}(M_I)$ that are larger than eq 20 by 5.7%. A simple modification to eq 20[34] employing a quadratic term in $\omega_{ex}/\gamma A_0$ leads to values of ω_{ex} that are essentially perfect up to $\omega_{ex}/\gamma A_0 = 0.41$ the highest value considered here.

For this study, it makes no practical difference whether I_{M_I} is allowed to vary or not since at the largest value of $\omega_{ex}/\gamma A_0 = 0.14$ the difference in the two methods is negligible. In this work, the lines are well separated even at the highest spin exchange frequency studied, and thus we were able to fit one line at a time using a fit window as before.[24] The advantage of this procedure is that error estimates are available from the deviations from line to line. In every case, fitting the entire spectrum yielded results equal to the results from fitting each line separately to within the uncertainties quoted below. In Table 2 , we give the upper limit of the value of $\omega_{ex}/\gamma A_0$ below which eqs 1, 20, 25, and 26 yield less than a 2% error in the determination of ω_{ex}. Table 2 shows that eqs 1, 20, 25, and 26 are accurate even at rather high values of $\omega_{ex}/\gamma A_0$.

Figure 2a shows a spectrum of PADS shortly after the beginning of the experiment which had a nominal concentration of 34 mM. The lines are broadened by 1.53 G above their limiting line widths at low concentrations. Even at this rather modest broadening, the distortion of the spectrum due to spin exchange is visually evident from the manner in which the spectrum appears to slope down and to the right. The entire line width of the center line is only 1.79 G, which means that the ratio of the line width to the hyperfine coupling constant is 0.136, well below of the limit of 0.3 established by Plachy and Kivelson[19] in which overlap of Lorentzian lines becomes a problem. Thus the non-Lorentzian nature of the spectrum is not due to overlap; it is due to the admixture of spin exchange dispersion discussed in connection with Figure 1. In Figure 2, the least-squares fit of eq 11 to the experimental spectrum is plotted over the experimental spectrum and is distinguishable only by its lack of noise. This is an example in which the entire spectrum was fit, allowing each I_{M_I} to vary independently. The excellent fit is illustrated in Figure 2b which is the difference in the experimental spectrum and the fit multiplied by 10. Figure 2d shows better detail of the fit to the one of the lines ($M_I = -1$) as well as the residuals. Figure 2c shows the least-squares fit to the $M_I = +1$ line using the Lorentzian shape showing that the Lorentzian is a rather poor description of the line shape even at this modest spin exchange broadening. Nevertheless, the Lorentzian fit does have the inherent advantages of spectral fitting and does provide surprisingly good values of the line position (needed to calculate A_{obs}) and the broadening. Fits of eq 11 to experimental spectra such as Figure 1a yield values of V_{disp}/V_{pp}, the line widths, and A_{abs} as was discussed in connection with Figure 1.

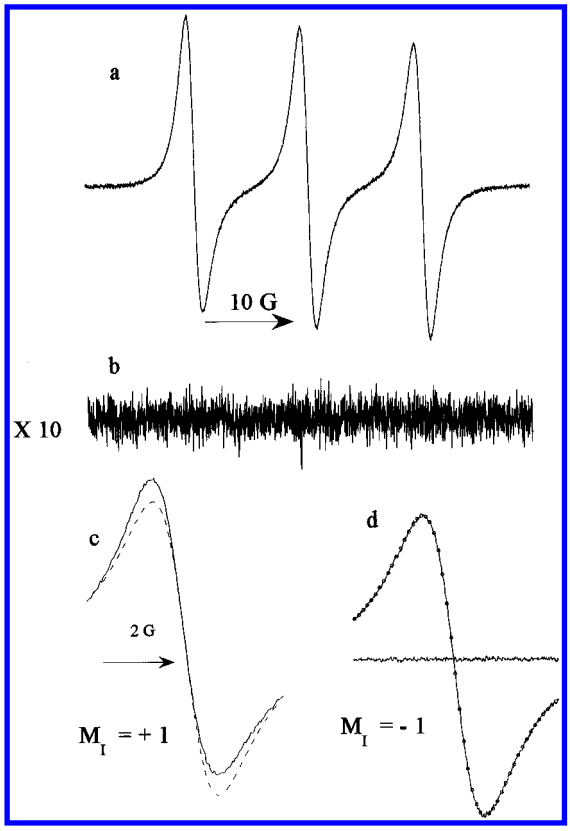

Figure 2. (a) EPR spectrum of PADS at 67 °C at a nominal concentration of 34 mM together with the fit of eq 17. (b) Ten times the difference in the best fit and the spectrum. (c) Best fit of a Lorentzian absorption to the $M_I = -1$ line and (d) the best fit of eq 17 to the $M_I = +1$ line with the residuals.

The doubly integrated intensity of an unsaturated EPR spectrum is proportional to the concentration of the radicals if all experimental parameters are held constant. In this experiment, the doubly integrated intensity was taken to be the value of I_{M_I} in the best fits of eq 11 to the spectra. This yields three values per spectrum, in arbitrary units, which were averaged.

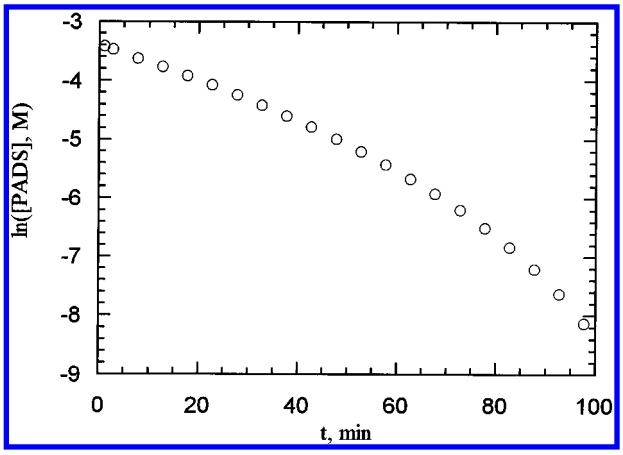

Figure 3. Natural logarithm of the molar concentration of PADS versus time.

The standard deviation of this average was less than 1% in all cases. In experiments with stable free radicals, we have found that spectral fitting yields reproducible values of the doubly integrated intensity to within 0.2−1% depending upon the signal-to-noise ratio if the sample is not disturbed. Removing and replacing the sample with care about doubles these uncertainties. In short, relative values of the intensity, which are of interest here, can be reproduced very well. Taking the extrapolation of the doubly integrated intensity back to zero time and dividing by the nominal concentration of the sample yields the constant of proportionality between the intensity and the concentration. Figure 3 shows the decay of the signal as a function of time at 67 ± 1 °C. The early portion of the decay shows approximate first-order kinetics, decaying more rapidly later; however, since the decay mechanism is immaterial to our purposes, no further investigation was made.

At low concentrations, it became possible to measure the Gaussian line width of 0.078 ± 0.008 G, 0.051 ± 0.004 G of which was induced by modulation broadening. The Lorentzian component of the line width was then computed using eq 7e of ref 22; the correction of the overall line width amounting to 0.02 G. With this correction, the linear extrapolation to zero concentration gave the following: $\Delta H^{L}_{pp}(0)_{+1} = 0.232 \pm 0.002$ G, $\Delta H^{L}_{pp}(0)_{0} = 0.234 \pm 0.002$ G, $\Delta H^{L}_{pp}(0)_{-1} = 0.236 \pm 0.002$ G, and $A_0 = 13.186 \pm 0.002$ G, the uncertainties being computed from the least-squares fitting in the usual way.[24]

The line broadenings were computed from eq 2. The broadening vs [PADS] is shown in Figure 4. The error bars on the broadening (a minor fraction of the size of the symbols) are the standard deviations derived from the values computed from the three lines. The absolute value of the concentration is uncertain by about 12%; however, as discussed above the relative values are precise to less than 1%. The solid line is a linear least-squares fit constrained to pass through the origin of coefficient of correlation $r = 0.999\,96$. Figure 4 provides a strong incentive to use spectral fitting methods: even for a rather small maximum broadening of about 1.4 G, extreme linear precision is obtained between theory of eqs 1 and 3 and experiment. Note that the maximum broadening in Figure 4 corresponding to $\omega_{ex}/\gamma A_0 = 0.11$ is well below the values at which the inner versus the outer lines would show different broadenings and is in fact low enough to be measured by any means including direct measurement (Table 2).

Allowing the parameters to vary independently for each line affords an opportunity to correct for normal dispersion. The amplitude of the dispersion for the $M_I = 0$ line is subtracted from those for the other two lines, leaving the contribution due to spin exchange. This yields two independent measurements

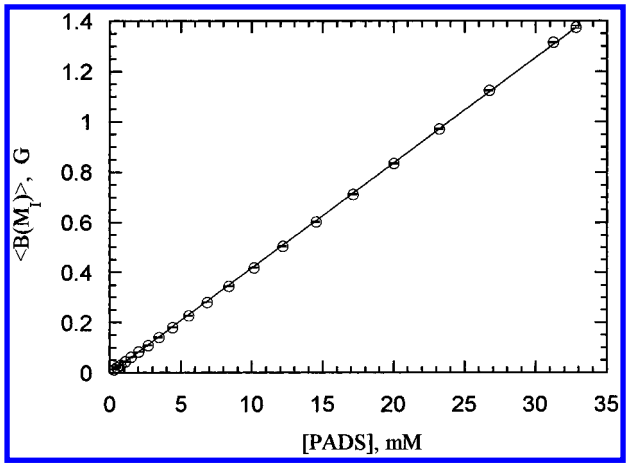

Figure 4. Spin exchange broadening of PADS averaged over the three lines versus the molar concentration of PADS. $T = 67$ °C. The error bars, small compared with the symbols, are the standard deviations in the results from the three lines. The solid line is a linear least-squares fit constrained to the origin with coefficient of correlation $r = 0.999\,96$.

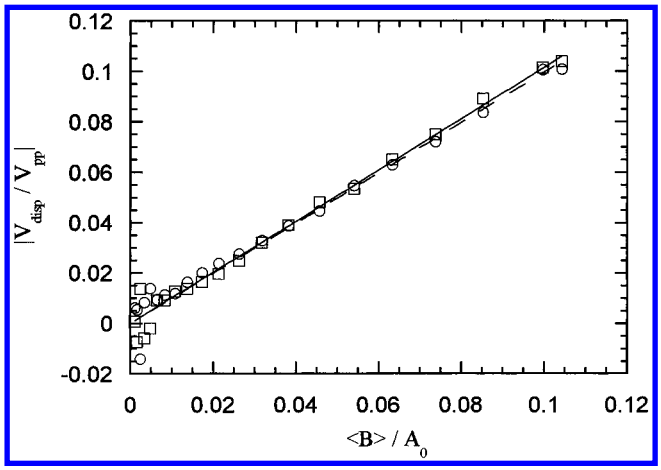

Figure 5. Absolute magnitude of the ratio of the amplitude of the dispersion component to the amplitude of the absorption component versus the ratio of the average broadening divided by the hyperfine coupling constant. Data derived separately from the $M_I = -1$ line (○) and from the $M_I = +1$ line (□) after having subtracted the amplitude ratio measured from the $M_I = 0$ line to correct for normal dispersion

of $|V_{disp}/V_{pp}|$ that ought to be equal to one another according to eq 20 and should be numerically equal to the broadening divided by A_0 according to eq 21. Figure 5 shows a plot of the two values of $|V_{disp}/V_{pp}|$ as a function of B/A_0. Except near the origin, where all of the measurements become uncertain, the two values of $|V_{disp}/V_{pp}|$ are very nearly equal, and their excellent correlation with B/A_0 is evident. The two lines (nearly coincident) are linear least-squares fits constrained to the origin having slopes 1.01 ± 0.02 and 0.997 ± 0.02, respectively. Figure 5 not only establishes the experimental validity of the formulation of spin exchange due to Molin et al.[4] but also shows that $|V_{disp}/V_{pp}|$ is a quite reasonable parameter to measure. The intriguing feature of $|V_{disp}/V_{pp}|$ is that it does not depend on a measurement at any other concentration. One does not need a sample at low concentration in order to estimate the spin exchange frequency.

The parameter A_{abs}/A_0 is plotted vs B/A_0 in Figure 6. The solid line is a plot of eq 25 employing no adjustable parameters, demonstrating that this aspect of the Molin et al.[4] theory is also supported by experiment. Figure 6 shows an extremely small effect; the error bars suppose an uncertainty in A_0 of 0.002 G and in A_{abs} of 0.004 G. The entire graph represents a shift of only 0.046 G, requires fitting spectra to eq 11, and clearly is

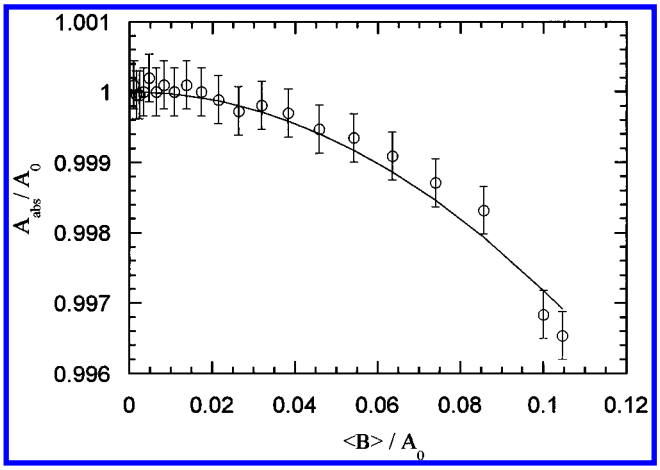

Figure 6. Variation of A_{abs} vs line broadening. Values of A_{abs}, not directly measurable from the spectra are found from least-squares fit of the spectra to eq 17. The error bars are computed using an uncertainty in the value of $A_0 = 0.002$ G and in $A_{abs} = 0.004$ G. The solid line is a plot of eq 25 with ω_{ex} calculated from eq 1; i.e., the curve has no adjustable parameters.

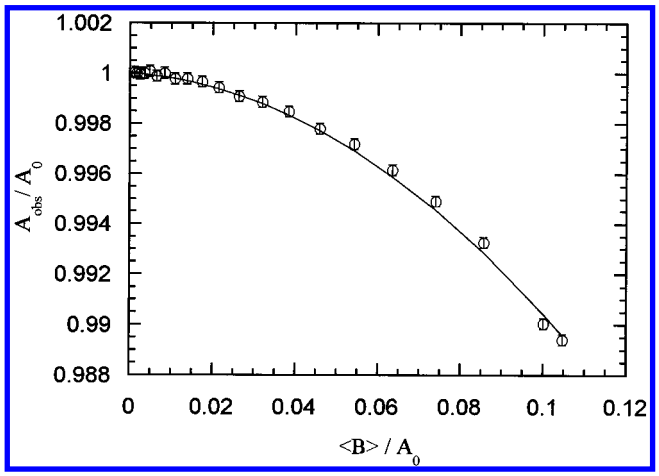

Figure 7. Variation of A_{obs} vs line broadening. Values of A_{obs} directly measurable from the spectra were found from a least-squares fit of the spectra to a Gaussian−Lorentzian sum approximation to a Voigt shape. Fits to Lorentzian lines or direct measurement gave the same results within experimental error. The error bars are computed using an uncertainty in the value of $A_0 = 0.002$ G and in $A_{obs} = 0.002$ G. The solid line is a plot of eq 26 with ω_{ex} calculated from eq 1; i.e., the curve has no adjustable parameters.

not a promising practical method to measure spin exchange frequencies.

Figure 7 shows the more straightforward parameter A_{obs}/A_0 plotted vs B/A_0. The solid line is a plot of eq 26 employing no adjustable parameters. The data for Figure 7 were obtained from a least-squares fit of the spectra to a Lorentzian−Gaussian sum function used as an approximate Voigt line shape as discussed previously;[24] however, direct measurements or fits to Lorentzian functions yield values that are indistinguishable from those in Figure 7 over this range of broadening.

According to eqs 1, 20, 25, and 26, spin exchange frequencies may be calculated from line broadening, line shifts, and the amplitude of the dispersion component. The results of these calculations are presented versus [PADS] in Figures 8 and 9. Figure 8 gives the results using broadening and the amplitude of the dispersion component. What appears to be a single solid line in Figure 8 is actually two linear least-squares fits to the two sources of information that are indistinguishable yielding $\omega_{ex}(B) = (9.568 \pm 0.013) \times 10^8$ s^{-1} M^{-1} ($r = 0.999\,96$) from broadening and $\omega_{ex}(V_{disp}) = (9.585 \pm 0.068) \times 10^8$ s^{-1} M^{-1} ($r = 0.998\,95$) from the dispersion amplitude, respectively. Clearly, both parameters give spin exchange frequencies in agreement with one another and linear with concentration. The surprising result is that measurement of V_{disp} yields results competitive in precision with the broadening without the ambiguity as to its origin. Figure 9 gives results derived from the two shifts, the solid symbols derived from A_{abs} and the open circles from A_{obs}. The error bars through the solid circles represent the uncertainties derived from the error bars in Figure 6, and the uncertainties in the open circles are about the size of the symbols. The solid and dashed lines are linear least-squares fits to ω_{ex} derived from A_{obs} and A_{abs} yielding $\omega_{ex}(A_{obs}) = (9.42 \pm 0.12) \times 10^8$ s^{-1} M^{-1} ($r = 0.9967$) and $\omega_{ex}(A_{abs}) = (9.34 \pm 0.26) \times 10^8$ s^{-1} M^{-1} ($r = 0.982$), respectively.

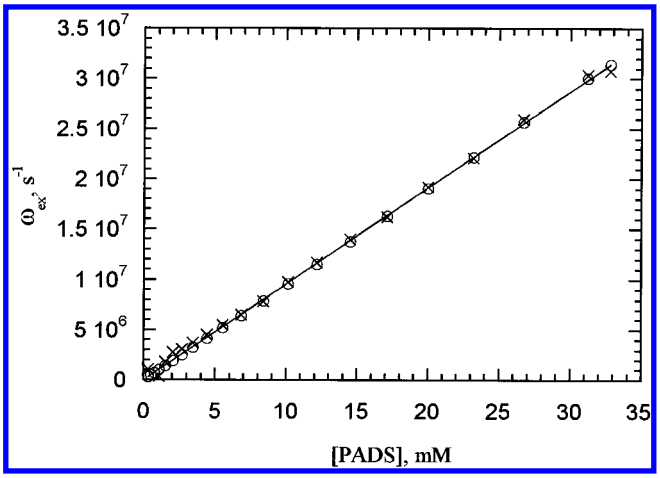

Figure 8. Spin exchange frequency versus the molar concentration of PADS as measured from line broadening (○) and from dispersion−absorption amplitude ratios (×). What appears to be a single solid line is actually two linear least-squares fits to the two sources of information that are indistinguishable yielding $\omega_{ex} = (9.568 \pm 0.013) \times 10^8$ s^{-1} M^{-1} ($r = 0.999\,96$) from line broadening and $\omega_{ex} = (9.585 \pm 0.068) \times 10^8$ s^{-1} M^{-1} ($r = 0.998\,95$) from dispersion−absorption amplitude ratios.

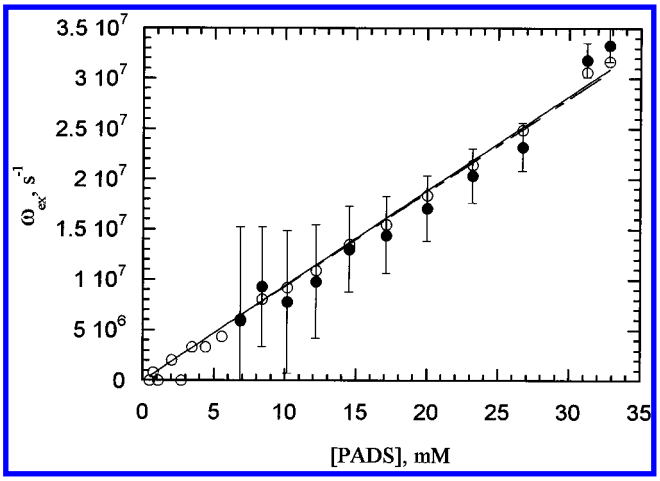

Figure 9. Spin exchange frequency versus the molar concentration of PADS as measured from A_{obs}/A_0(○) and from A_{abs}/A_0 (●). The solid line is a linear least-squares fit to the data derived from A_{obs}/A_0 yielding $\omega_{ex} = (9.42 \pm 0.12) \times 10^8$ s^{-1} M^{-1} ($r = 0.9967$), and the broken line is a fit to the data derived from A_{abs}/A_0 yielding $\omega_{ex} = (9.34 \pm 0.26) \times 10^8$ s^{-1} M^{-1} ($r = 0.9817$).

Discussion

Using the theory of Molin et al.,[4] we have derived an analytical expression, eq 11 or 17, for the EPR line shape of a nitroxide free radical undergoing spin exchange. This expres-

sion applies to spectra motionally narrowed by rotational motion, and although derived for the slow exchange limit, $\omega_{ex} \ll \gamma A_0$, it was found to yield precise values of ω_{ex} up to rather large values of $\omega_{ex}/\gamma A_0$. For example, if I_{M_I} is constrained to be independent of M_I, then ω_{ex} is precise to within 2% up to values of $\omega_{ex}/\gamma A_0 = 0.21(A_{abs})$, $0.29(V_{disp})$, and $0.41(\langle B_{M_I}\rangle)$ when the parameter used to determine ω_{ex} is indicated in the parentheses. By allowing I_{M_I} to vary with M_I, and modifying eq 20,[34] essentially perfect results are obtained up to the limit considered here, $\omega_{ex}/\gamma A_0 = 0.41$, with every indication that this limit may be extended even higher. The expression is simple: a sum of a Lorentzian absorption and dispersion whose relative magnitudes are a linear function of ω_{ex}.

The significance of the validity of the new analytic expression is 2-fold: (1) an analytic expression is now available that may be used to perform nonlinear least-squares fits of experimental spectra allowing rather noisy spectra to be analyzed accurately. This is of particular importance in applications in which a limited amount of sample is available and/or the concentration of the nitroxide free radical is kept low. Even in experiments of high signal-to-noise ratios, the automated processing of data afforded by spectral fitting is a tremendous time saver. (2) A new, independent method to derive ω_{ex} is now available from the measurements of V_{disp}. This parameter may be measured with precision comparable to that of the line broadening and is not dependent upon measurements at any other concentration.

The validity of eq 24 expressing the relationship between ω_{ex} and the observed line shifts was shown theoretically and experimentally. This taken together with Jones' observations[3] that the modified Bloch equations also yield excellent agreement between values of ω_{ex} derived from line broadening and line shifts demonstrates that the modified Bloch equations and more rigorous theories are in agreement on this point. The analytic expression, eq 24, offers obvious advantages to the transcendental equation given by Jones[3] that must be solved numerically. In addition, a nonzero line width in the absence of spin exchange may be included.

Fitting of theoretical and experimental spectra to eq 11 or 17 allowed a determination of A_{abs} and confirmation of the validity of eq 25 for the first time.

Line broadening is found to be accurately (2% level) predicted by eq 1 up to $\omega_{ex}/\gamma A_0 = 0.17$ when the broadening is directly measured from the spectrum, provided the average broadening is used. Spectral fitting, either allowing I_{M_I} to vary or not, yields broadenings accurately given by eq 1 up to $\omega_{ex}/\gamma A_0 = 0.41$, the highest value studied. Interestingly, spectral fitting using the Lorentzian line shape which is clearly incorrect, yields accurate broadenings up to $\omega_{ex}/\gamma A_0 = 0.31$. There is no reason to fit to a Lorentzian rather than the correct expression, eq 11 or 17; however, fitting software is already available in many labs, and if this software is used, accurate values of the broadening may be obtained up to the limit given in Table 2. Further, A_{obs} is found directly from a fit to a Lorentzian or a Voigt, which is not directly available from a fit to eq 11 or 17.

The preponderance of information from spin exchange experiments has been derived from line broadening because it is a simple measurement. There are cases in which line broadening is not straightforward to analyze, however, and other sources of information become useful. For example, at low spin exchange frequencies, i.e., those of the most interest in which only modest concentrations of nitroxides may be tolerated (for example, biological systems) broadening is not a sensitive function of concentration for nitroxide spin probes with significant unresolved hyperfine structure. See Figures 3 and 4 of ref 35. In biological applications, the doxyl-labeled fatty acids and phospholipids are some of the most widely used probes, and these are nitroxides whose line width is dominated by inhomogeneous broadening due to unresolved hyperfine structure.[22] The same is true of 3-carboxyproxyl.[36] Further work will be needed to extend the type of line-shape measurements described here to these types of nitroxides.

The study of complex liquids is another example in which the line widths do not provide a straightforward source of information. In complex liquids, for example micelles, nitroxides are distributed statistically among compartments, and the resulting spectrum is the superposition of spectra due to compartments, containing one, two, three, etc., nitroxides.[37−41] In these complex liquids, the line width is no longer linear with the concentration. In many cases the line width is fairly insensitive to the spin exchange frequency; in fact, in some realistic cases, the observed line width is expected to *decrease* with increasing spin exchange frequency. The reason for this odd behavior is that singly occupied compartments, which are not affected by spin exchange, can dominate the spectra and therefore the line widths.

Finally, both dipolar and spin exchange interactions broaden the lines linearly with the radical concentration. To derive information on the translational diffusion of the radicals, the effect of these two interactions must be separated. In the past, the temperature dependence of the concentration broadening was studied[10] relying upon a Stokes−Einstein model (eq 4) to separate the two interactions. This approach often worked with simple liquids because the shear viscosity could be determined from other experiments; however, Berner and Kivelson[10] were pessimistic about the usefulness of spin exchange line broadening in higher viscosity media such as biological membranes. By studying the amplitude of the spin exchange induced dispersion and the line shifts, one may may be able to focus only upon the spin exchange contribution. Experiments will need to be performed in viscous liquids to verify that spin exchange and dipolar interactions may be separated.

The results presented here apply to nitroxides with inhomogeneous line broadening that may be neglected. If this is not the case, the effect of unresolved hyperfine structure will need to be included, i.e., if $\omega_{ex} \approx \gamma A_{eff}$ where A_{eff} is the effective hyperfine coupling that produces the unresolved structure. This will become important if rather small values of ω_{ex} are to be studied. It appears that with minor modifications one may study the other extreme when ω_{ex} is large, perhaps rather near to the intermediate spin exchange case $\omega_{ex} \approx \gamma A_0$.

Conclusions

An analytical expression for the line shape of a nitroxide free radical undergoing spin exchange in the slow exchange limit was derived which is the sum of first-derivative Lorentzian absorption and dispersion lines centered at the same resonance field. The validity of the line shape in every detail was determined by comparison with the theory of Currin[6] and experimentally verified. The relative amplitudes of the absorption and dispersion components is a linear function of the spin exchange frequency for slow spin exchange. This ratio may be measured with good precision using nonlinear least-squares fitting of the spectra yielding an independent value of the spin exchange frequency competitive in precision with values derived from line broadening and not dependent upon measurements at low concentration. The resonance fields of the outer lines shift toward the center of the spectrum as the square of the spin exchange frequency (eq 23) and the observed positions of the Lorentzian absorption−dispersion admixtures shift further, also as a quadratic function of the spin exchange frequency (eq 24).

The observed shift also involves the unbroadened Lorentzian line width (eq 24). Both shifts may be used to measure the spin exchange frequency; however, only the observed shift yields values that are of precision comparable with broadening and dispersion-amplitude techniques.

Appendix

The line shape is given by the real part of the first derivative of the Currin expression,[6] which, including different line widths for each line is given by

$$G(H) = \frac{S(H)}{1 - (\omega_e/\gamma)S(H)} \tag{27}$$

where H is the magnetic field, ω_e the spin exchange frequency, γ the gyromagnetic ratio of the electron, and $S(H)$ is given by

$$S(H) = \sum \frac{\rho_j}{i(H - H_j) + \gamma^{-1}[\omega_e + (T_2^{-1})_j]} \tag{28}$$

In eq 28, $i = \sqrt{-1}$ and the sum is over j which denotes the jth resonance line in the spectrum which appears at resonance field H_j, with degeneracy ρ_j, and is characterized by spin−spin relaxation time $(T_2)_j$. The peak-to-peak first-derivative Lorentzian line width of the jth line is given by $\Delta H_{pp}^{L})(0)_j = 2\gamma^{-1}(T_2^{-1})_j/\sqrt{3}$.

The observed EPR spectrum is found by taking the real part of the first derivative of eq 27 yielding

$$Y'(H) = \frac{DN' - ND'}{D^2} \tag{29}$$

In eq 29,

$$N = S(H)_2\left(1 - \frac{\omega_e}{\gamma}S(H)_2\right) - \frac{\omega_e}{\gamma}S(H)_1{}^2$$

$$D = \left(1 - \frac{\omega_e}{\gamma}S(H)_2\right)^2 + \left(\frac{\omega_e}{\gamma}S(H)_1\right)^2$$

$$N' = -2S(H)_5 + 4\frac{\omega_e}{\gamma}S(H)_2S(H)_5 - 2\frac{\omega_e}{\gamma}S(H)_1(S(H)_3 - 2S(H)_4)$$

$$D' = 4\frac{\omega_e}{\gamma}S(H)_5\left(1 - \frac{\omega_e}{\gamma}S(H)_2\right) + 2\left(\frac{\omega_e}{\gamma}\right)^2 S(H)_1(S(H)_3 - 2S(H)_4)$$

with the following definitions:

$$\Omega_j = \gamma^{-1}[\omega_e + (T_2^{-1})_j]$$

$$L_j(H) = 1/[(H - H_j)^2 + (\Omega_j)^2]$$

the sums are as follows:

$$S(H)_1 = \sum \rho_j(H - H_j)L_j(H)$$

$$S(H)_2 = \sum \rho_j\Omega_jL_j(H)$$

$$S(H)_3 = \sum \rho_jL_j(H)$$

$$S(H)_4 = \sum \rho_j(H - H_j)^2[L_j(H)]^2$$

$$S(H)_5 = \sum \rho_j\Omega_j(H - H_j)[L_j(H)]^2$$

All of the sums extend over all of the lines of the spectrum.

Acknowledgment. This research was supported by grants from the NIH/MBRS S06 GM48680-03 (to B.L.B.), NIH 1 R15 GM/HL51103-01A1 (to B.L.B.), NIH 3 R15 GM/RR494737-01S1 (to M.P.) and grants from the CSUN Research and Grants Committee (to B.L.B. and M.P.).

References and Notes

(1) Kivelson, D. *J. Chem. Phys.* **1960**, *33*, 1094.
(2) Freed, J. H. *J. Chem. Phys.* **1966**, *45*, 3452.
(3) Jones, M. T. *J. Chem. Phys.* **1963**, *38*, 2892.
(4) Molin, Y. N.; Salikhov, K. M.; Zamaraev, K. I. *Spin Exchange. Principles and Applications in Chemistry and Biology*; Springer-Verlag: New York, 1980; Vol. 8.
(5) Salikhov, K. M.; Doctorov, A. B.; Molin, Y. N.; Zamaraev, K. I. *J. Magn. Reson.* **1971**, *5*, 189.
(6) Currin, J. D. *Phys. Rev.* **1962**, *126*, 1995.
(7) Ayant, Y.; Besson, R.; Salvi, A. *J. Phys.* **1975**, *36*, 571.
(8) Johnson Jr., C. S. *Mol. Phys.* **1967**, *12*, 25.
(9) Stillman, A. E.; Schwartz, L. J.; Freed, J. H. *J. Chem. Phys.* **1980**, *73*, B1.23.
(10) Berner, B.; Kivelson, D. *J. Phys. Chem.* **1979**, *83*, 1406.
(11) Kovarskii, A. L.; Wasserman, A. M.; Buchachenko, A. L. *J. Magn. Reson.* **1972**, *7*, 225.
(12) Eastman, M. P.; Kooser, R. G.; Das, M. R.; Freed, J. H. *J. Phys. Chem.* **1969**, *71*, 38.
(13) Eastman, M. P.; Bruno, G. V.; Freed, J. H. *J. Chem. Phys.* **1970**, *52*, 2511.
(14) King, M. D.; Sachse, J. H.; Marsh, D. *J. Magn. Reson.* **1987**, *72*, 257.
(15) Sachse, J. H.; King, M. D.; Marsh, D. *J. Magn. Reson.* **1987**, *71*, 385.
(16) Martini, G.; Bindi, M. *J. Colloid Interface Sci.* **1985**, *108*, 133.
(17) Miller, T. A.; Adams, R. N.; Richards, P. M. *J. Chem. Phys.* **1966**, *44*, 4022.
(18) Nayeem, A.; Rananavare, S. B.; Sastry, V. S. S.; Freed, J. H. *J. Chem. Phys.* **1989**, *91*, 6887.
(19) Plachy, W.; Kivelson, D. *J. Chem. Phys.* **1967**, *47*, 3312.
(20) Wertz, J. E.; Bolton, J. R. *Electron Spin Resonance. Elementary Theory and Practical Applications*; Chapman and Hall: New York, 1986.
(21) Kubo, R.; Tomita, K. *J. Phys. Soc. Jpn.* **1954**, *9*, 888.
(22) Bales, B. L. Inhomogeneously Broadened Spin-Label Spectra. In *Biological Magnetic Resonance*; Reuben, L. J. B. a. J., Ed.; Plenum: New York, 1989; Vol. 8, 77.
(23) Smirnov, A. I.; Belford, R. L. *J. Magn. Reson. A* **1995**, *113*, 65.
(24) Halpern, H. J.; Peric, M.; Yu, C.; Bales, B. L. *J. Magn. Reson. A* **1993**, *103*, 13.
(25) Peric, M.; Halpern, H. J. *J. Magn. Reson. A* **1994**, *109*, 198.
(26) Bales, B. L. *J. Magn. Reson.* **1980**, *38*, 193.
(27) Bales, B. L. *J. Magn. Reson.* **1982**, *48*, 418.
(28) Bales, B. L.; Willett, D. *J. Magn. Reson.* **1983**, *51*, 138.
(29) Eastman, M. P. *J. Chem. Educ.* **1982**, *59*, 677.
(30) Fraenkel, G. K. *J. Chem. Phys.* **1965**, *42*, 4275.
(31) Sueki, M.; Rinard, G. A.; Eaton, S. S.; Eaton, G. R. *J. Magn. Reson.* **1996**, *A118*, 173.
(32) Slichter, C. P. *Principles of Magnetic Resonance*, 3rd ed.
(33) Bales, B. L.; Wajnberg, E.; Nascimento, O. R. *J. Magn. Reson.* **1996**, *A 118*, 227.
(34) Bales, B. L.; Peric, M., unpublished results, 1997.
(35) Bales, B. L.; Willett, D. *J. Chem. Phys.* **1984**, *80*, 2997.
(36) Bales, B. L.; Peric, M.; Lamy-Freund, M. T., unpublished results, 1997.
(37) Persson, K.; Bales, B. L. *J. Chem. Soc., Faraday Trans.* **1995**, *91*, 2863.
(38) Bales, B. L.; Stenland, C. *J. Phys. Chem.* **1993**, *97*, 3418.
(39) Bales, B. L.; Stenland, C. *J. Phys. Chem.* **1995**, *99*, 15163.
(40) Aizawa, M.; Komatsu, T.; Nakagawa, T. *Bull. Chem. Soc. Jpn.* **1980**, *53*, 975.
(41) Sankaram, M. B.; Marsh, D.; Thompson, T. E. *Biophys. J.* **1992**, *63*, 340.